Published in final edited form as:

J Biomed Mater Res B Appl Biomater. 2016 July ; 104(5): 864–879. doi:10.1002/jbm.b.33438.

Keratin hydrogel carrier system for simultaneous delivery of exogenous growth factors and muscle progenitor cells[1,,2,,3]

Seth Tomblyn[1], **Elizabeth Pettit Kneller**[1], **Stephen J. Walker**[2], **Mary D. Ellenburg**[1], **Christine J. Kowalczewski**[3,4], **Mark Van Dyke**[3], **Luke Burnett**[1], and **Justin M. Saul**[4]

[1]KeraNetics, LLC, Suite 168, 391 Technology Way, Winston-Salem, NC 27101

[2]Wake Forest Institute for Regenerative Medicine, Wake Forest University Health Sciences, Winston-Salem, NC 27157

[3]Virginia Tech-Wake Forest University School of Biomedical Engineering and Sciences, Blacksburg, VA 24061

[4]Department of Chemical, Paper, and Biomedical Engineering, Miami University, Oxford, OH 45056

Abstract

Ideal material characteristics for tissue engineering or regenerative medicine approaches to volumetric muscle loss (VML) include the ability to deliver cells, growth factors and molecules that support tissue formation from a system with a tunable degradation profile. Two different types of human hair-derived keratins were tested as options to fulfill these VML design requirements: (1) oxidatively extracted keratin (keratose) characterized by a lack of covalent crosslinking between cysteine residues, and (2) reductively extracted keratin (kerateine) characterized by disulfide crosslinks. Human skeletal muscle myoblasts cultured on coatings of both types of keratin had increased numbers of multinucleated cells compared to collagen or Matrigel™ and adhesion levels greater than collagen. Rheology showed elastic moduli from 10^2 – 10^5 Pa and viscous moduli from 10^1 – 10^4 Pa depending on gel concentration and keratin type. Kerateine and keratose showed differing rates of degradation due to the presence or absence of disulfide crosslinks, which likely contributed to observed differences in release profiles of several growth factors. In vivo testing in a subcutaneous mouse model showed that keratose hydrogels can be used to deliver mouse muscle progenitor cells and growth factors. Histological assessment showed minimal inflammatory responses and an increase in markers of muscle formation.

Keywords

tissue engineering; regenerative medicine; controlled release; hydrogel; growth factor

[1]The author, or one or more of the authors, has received or will receive remuneration or other prequisites for personal or professional use from a commercial or industrial agent in direct or indirect relationship to their authorship. (ST, EPK, MDE, CJK, MVD, LB)

[2]The benefits accruing to the author or authors from a commercial or industrial party will be applied to a research fund, nonprofit institution or other organization with which the author(s) are associated. (CJK, JMS)

[3]No benefit of any kind will be received either directly or indirectly by the author(s). (SJW)

Corresponding Author: Justin M. Saul, Current address: Department of Chemical, Paper, and Biomedical Engineering, Miami University, 650 East High Street, Room 064L, Oxford, OH 45056. sauljm@MiamiOH.edu. Ph.: 513-529-0769. Fax: 513-529-0761.

1. Introduction

Current strategies for tissue engineering and regenerative medicine (TERM) consist of delivering the triad of cells, materials and growth factors for the repair of multiple tissues including bladder [1], trachea [2], bone [3], and others [4–6]. One area of particular need of TERM strategies is injury to muscle tissue and, in particular, for volumetric muscle loss (VML) due to a lack of treatment modalities. Skeletal muscle injuries are common due to trauma in both civilian and military populations [7]. In 2004, the total estimated cost to the U.S. Healthcare system (including lost wages) associated with musculoskeletal diseases was $949 billion [8]. Specific information regarding the incidence of skeletal muscle injuries is difficult to determine, but it has been reported that injury treatment for sprains, strains, contusions, and open wounds accounts for 63% of injury treatment episodes [9]. Although autologous tissues are the “gold standard” in treatment of several other types of tissue injury (e.g., bone and skin grafts), there are only a few approaches to the use of autografts in volumetric muscle loss injuries including free or vascularized flaps [10] and minced muscle grafts [11]. Each type leads to a deficit in another location, and there are therefore limited locations that can be used. Therefore, TERM-treatment strategies offer an alternative that does not create a donor site deficit.

Considerable progress toward *de novo* skeletal muscle formation has been made through the use of bioreactor technology [12]. However, this approach has only resulted in thin muscle sheets or small volumes of tissue, both of which are not suitable for VML treatment in adult humans. A potential solution could be the development of new materials that support tissue formation *in situ* through controlled degradation of a TERM construct that can deliver cells and provide controlled release of bioactive molecules. Synthetic polymers can be tailored to achieve desirable degradation profiles or rates of growth factor delivery, but it has long been known that additional modifications are necessary to promote improved cell attachment [13,14]. While such approaches are being used to better understand and direct cell behavior [15–17], degradation products of some synthetic materials have been associated with inflammatory and foreign body responses in certain conditions [18–20]. Some naturally-based materials such as the polysaccharide alginate can persist for long periods of time *in vivo*, but like synthetic polymers require modification in order to have tunable rates of degradation or present cell-binding motifs that cells would encounter in the three-dimensional environment [21,22].

Collagen is perhaps the most widely used natural polymer used in TERM application due to its natural degradation products and inherent ability to promote cell attachment [23,24]. However, collagen is not well suited to the controlled temporal delivery of exogenous agents such as growth factors because collagenous materials degrade rapidly, particularly in the presence of collagenase or other protein-specific enzymes [25,26]. The rapid degradation profile of collagen requires moderately complex modifications in order to avoid poor tissue structure associated with loss of the scaffolding material[27,28]. Nonetheless, protein derived-natural polymers that promote cell attachment and offer cell/tissue compatibility are of considerable interest for TERM applications.

Indeed, a number of such protein-based natural polymers have been or are being investigated either alone or in combination with existing materials. Examples include silk [29], fibrin [30], elastin [31], and soy proteins [32]. Another potential system to overcome limitations with existing natural polymer carrier systems are keratin biomaterials. Keratin proteins have some advantages of both natural and synthetic polymer systems that make their use for TERM applications potentially advantageous. As a natural, protein-derived polymer, keratins have cell binding motifs in their primary protein structure [33] and promote attachment and growth of cells through mechanisms that are only beginning to be elucidated [34]. Keratins are characterized by a relatively high cysteine residue content, providing the potential for flexible chemistry reminiscent of synthetic polymers when appropriate types of extraction are used (see below). Unlike collagen and some other naturally-derived proteins, to our knowledge humans do not produce enzymes that specifically degrade keratins (i.e., keratinases), which allows these materials to persist *in vivo* for longer periods of time. Lastly, in terms of controlled release, we have previously suggested [35,36] that release of therapeutic agents from keratin biomaterials is related to adsorption affinity of these materials to keratin and therefore release is not simply diffusion-mediated.

Based in part on these advantageous properties, keratin has previously been investigated for various TERM applications including nerve regeneration [37–40], bone tissue formation [41], wound healing in skin [42], and even myocardial infarction[43]. Keratins can be extracted from several sources including wool [44,45], feathers [46] and, in the work reported here, human hair [47,48]. Two primary methods of human hair keratin extraction have been reported, as shown schematically in Figure 1A [49]. One process uses oxidative chemistry to produce keratin proteins that are known as keratose [50]. Another process uses reductive chemistry to produce keratin proteins that are referred to as kerateine [51]. Keratose (KOS) is characterized, in part, by the oxidation of cysteine residues to sulfonic acid, which prevent covalent disulfide cross-links from re-forming (Figure 1, left side). Cysteine residues in kerateine (KTN) are able to form disulfide cross-links (Figure 1, right side). Both KOS and KTN can form hydrogels, but the chemical structure of each suggests that KOS polymerizes via chain entanglements (non-covalent cross-links) while KTN polymerizes via both chain entanglement and covalent cross-links. These forms of keratin (KOS and KTN) have distinct mechanical and chemical properties. Additional variation in the material properties of keratin formulations can be achieved by varying the amounts of high molecular weight/lower sulfur content alpha (α) proteins or low molecular weight/high sulfur content gamma (γ) proteins obtained by sub-fraction of the KOS and KTN extracts.

It has been shown previously, that keratin hydrogels (KOS or KTN) can support the controlled release of antibiotics [36] and bone morphogenetic protein 2 (rhBMP-2) [35,52]. These studies showed that the rates of release correlated with the rate of KOS or KTN degradation. Because the rate of keratin degradation depends on the types of crosslinks, KOS [50] showed more rapid degradation than KTN [51]. It was therefore hypothesized that degradation rate could be used to control the rate of delivery of therapeutic growth factors by manipulation of the type of keratin gel. This would, in turn, provide a platform with characteristics of both natural (e.g., cell attachment and synthetic (e.g., controlled release and degradation) polymers.

We tested the ability of keratin biomaterials to serve the key functions of the TERM triad: material, cell delivery, and growth factor (signal) delivery. In order to determine the optimal features of a keratin TERM system for VML, four experiments were conducted. The first experiment examined skeletal muscle precursor cell growth and attachment on keratin coatings. The second experiment used three-dimensional keratin hydrogels to examine delivery of individual or combinations of several growth factors relevant to skeletal muscle regeneration as a cocktail. The third experiment tested the ability of keratin carriers to support delivery of viable cells in combination with growth factors. The fourth experiment assessed selected formulations containing cells and or growth factors implanted in a subcutaneous mouse model.

2. Materials and Methods

2.1. Materials

Human hair was obtained by KeraNetics, LLC from World Response Group. VEGF, high binding plates for ELISAs, VEGF ELISA kit, and IGF-1 ELISA kit were obtained from R&D Systems (Minneapolis, MN). IGF-1, bFGF, and bFGF ELISA were obtained from Peprotech (Rocky Hill, NJ). C57BL/6J mice were obtained from Harlan Laboratories (Indianapolis, IN). Ascorbic acid, EDTA, Triton-X100, 28% ammonium hydroxide, Tween 20, and reagents for hematoxylin and eosin (H&E) staining were from Sigma-Aldrich (St. Louis, MO). Horse serum, fetal bovine serum (FBS), high glucose DMEM, low glucose DMEM, DMEM/F12, chick embryo extract, and PBS were obtained from Invitrogen/Life Technologies (Grand Island, NY). Matrigel™ was obtained from BD Biosciences (San Jose, CA). The Lavacell assay for live cells was from ActiveMotif (Carlsbad, CA). Antibody and immunohistochemical staining kit for blood vessels (von Willebrand factor) was obtained from Millipore (Billerica, MA). Antibody for desmin staining was obtained from Santa Cruz Biotechnology (Santa Cruz, CA). Secondary antibody for HRP staining of desmin was obtained from Vector Laboratories (Burlingame, CA). DC Protein Assay for the modified Lowry method of total protein content was obtained from Bio-Rad (Hercules, CA). Type I collagen was obtained from Worthington Biochemical (Lakewood, NJ).

2.2. Keratin preparation

Keratins were extracted by using a proprietary patent-pending process in a Quality Systems Regulated facility at KeraNetics, LLC in a manner similar to those previously published[36,37]. Consistent with these previous reports, the non-proprietary parts of the extraction process are described here briefly. A cold solution of 0.5M thioglycolic acid (TGA) in sodium hydroxide (reductive extraction for KTN) or a 2% peracetic acid (PAA) solution (oxidative extraction for KOS) were added to chopped human hair. For reductive extraction, the reducing solution was added to hair in a mixing tank for 12 hours at 37°C followed by two washes in 100mM Tris base and water. The solution was then centrifuged, filtered, dialyzed against a 100 kDa molecular weight cutoff cellulose membrane, and neutralized to pH 7.4. For oxidative extraction with PAA, the hair was processed in a similar manner. Following PAA or TGA extraction, acid precipitation of the alpha fraction, centrifugation, re-dissolution in buffer, and dialysis in water with a 30 kDa nominal low molecular weight cutoff membrane were performed. The supernatant containing the gamma

fraction (low molecular weight/high sulfur content proteins) was filtered, neutralized to pH 8.0 and dialyzed against a 3 kDa low molecular weight membrane to separate from the alpha proteins (high molecular weight/lower sulfur content). The resulting solutions were lyophilized, ground, and sterilized by 2Mrad gamma irradiation.

2.3. Characterization of human skeletal muscle myoblast response to keratin coatings

The response of muscle cells to keratin materials was initially characterized by culturing human skeletal muscle myoblasts (hSMM; Lonza, Walkersville, MD) on uncoated tissue culture polystyrene (TCPS) or TCPS coated with keratin or two other common protein-based cell culture coatings: collagen or Matrigel™ These experiments determined cell adhesion, cell proliferation, Giemsa staining for visualizing cell morphology and nucleation, and gene expression by micro-array analysis in response to one keratin coating of interest (gamma KOS).

Cell Culture and Coatings—hSMM were plated at 3500 cells/cm^2 in SKGM-2® medium, with a media change the day after plating. Once the cells reached approximately 60% confluence, one half of the media was removed and replaced with an equal volume of fresh media, every other day. Uncoated TCPS plates were used as controls.

Giemsa staining—Giemsa staining was performed by fixing cells in methanol for 5 minutes, followed by 25 minutes of staining in Giemsa (Sigma, St. Louis, MO), and two brief rinses in distilled/deionized water according to the manufacturer's instructions. Images were collected with a TCA 9.0 MP camera (Tucsen, Fujien, China) attached to a Nikon Diaphot microscope using the TSView Software version 7.1.0.4 (Tucsen, Fujien, China). The percentage of multi-nucleated cells was determined by counting 20 different fields and pair-wise student t-tests were used to determine statistical differences between groups with $p < 0.05$ taken to be statistically significant. Counts were conducted by two trained but blinded observers, and results for each field were averaged.

Adhesion and Proliferation—Adhesion assays were performed by using the Vybrant® assay kit (Molecular Probes, Eugene OR) according to the manufacturer's instructions in black-walled clear bottom 96-well plates at 2 hours after seeding the cells. The number of cells required for seeding (75,000 cells/well) was determined on uncoated plates prior to testing with different coatings. Fluorescence was detected with a Molecular Devices SpectraMax Gemini EM plate reader at excitation/emission of 485/538 nm. The percent adhesion was determined by dividing the fluorescence of adherent cells following four washes by the total fluorescence of unwashed cells. To correct for background fluorescence from each coating, which was minimal, the fluorescence from wells containing no cells was subtracted.

Proliferation assays were performed by using the Cell Titer-Glo® assay (Promega, Madison, WI). Cells were seeded at a density of 5000 cells/cm^2 in 48 well plates and at the indicated times post-seeding, cells were assayed according to the manufacturer's instructions, by randomizing the samples in white-walled 96-well plates for luminescence readings (Molecular Devices plate reader).

2.4. Hydrogel formation and rheological characterization

After evaluating cellular response to two-dimensional coatings, three-dimensional keratin hydrogel constructs were investigated. To form keratin hydrogels, water was added to dry keratin powders at the desired weight percent (per unit volume). KOS gels were prepared at 12 or 20% (w/v) and KTN hydrogels were prepared at 8 or 20%. 20% gels are described to allow direct comparison between KOS and KTN while the 8% KTN and 12% KOS are described as these were the final formulations selected for in vitro and in vivo experiments involving keratin hydrogels and muscle progenitor cells. In addition to the weight percentages described, other formulations (of different weight percentages) were screened by rheology, but not included if they didn't meet design criteria (see Results 3.2).

Rheological testing was conducted on a Bohlin CS10 rheometer (Malvern, Worcestershire, UK) in a plate-plate configuration. A 1 mm thick section of each keratin hydrogel (n = 3) was placed on the lower plate. After an initial stress sweep at 1Hz (rad/s), an oscillatory stress of 25 Pa was selected for frequency sweep experiments over the range of 0.01 – 10Hz. Values for G', G'', tan δ, and other mechanical properties were determined as a function of frequency over this range.

2.5. *In vitro* determination of keratin degradation and VEGF, IGF-1, and bFGF release

For growth factor experiments, keratin hydrogels were formed as described above and hydrated with a growth factor-water solution. Growth factors were diluted in sterile water at neutral pH to yield 100 μg/mL of bFGF, 100 μg/mL of IGF-1, or 10 μg/mL of VEGF per 100 μL gel, giving masses of 10 μg bFGF, 10 μg IGF-1 or 1 μg VEGF in each gel. The concentrations of growth factors were varied to account for differences in their potencies. Growth factor solutions were then added to KOS or KTN powders and thoroughly mixed by vortexing. The resulting keratin hydrogels were varied by adjusting the weight:volume (w/v) ratio to values of 20% (KOS and KTN), 12% (KOS), or 8% (KTN).

One hundred μL aliquots of the keratin hydrogel/growth factor mixtures were placed into separate sterile 1.5 mL micro-centrifuge tubes and the hydrogels were allowed to gel overnight at 37°C. The hydrogels were then overlaid with 100 μL of sterile PBS. The PBS was removed and replaced at 1.5, 3, 6, 12, and 24 hours, 2, 3, 4, 5, 6, and 7 days, 2, 3, and 4 weeks. Samples were stored at −20 °C until quantification. Total protein (primarily measuring erosion of the keratin gels because the amount of protein growth factor is small compared to the amount of keratin [36,50,51]) was determined via Lowry assay (Bio-Rad) according to the manufacturer's instructions. Growth factor concentrations were determined by ELISA (R&D and Peprotech) per manufacturer's instructions with the exception of using carbonate buffer (100 mM Bicarbonate/carbonate, pH 9.6) to plate the capture antibody.

2.6. Myoblast progenitor cell isolation

The ability of keratin hydrogels (with or without growth factors) to act as a carrier system for muscle progenitor cells was also tested. For these studies, the goal was to produce a viable formulation that could eventually be tested in an *in vivo* mouse model using isogeneic cells. This approach is comparable to those that are employed clinically using autologous cells. In order to use a non-immunocompromised mouse model, primary myoblast

progenitor cells were used in lieu of hSMM cells used in the initial *in vitro* tests described above. Primary myoblast progenitor cells were obtained from C57BL/6 donor mice (2–4 weeks of age) for implantation into experimental (20 gram) C57BL/6 mice (an inbred strain to allow use of isogenic cells) in a manner described previously for rats [12,53]. All animal work was approved by the Wake Forest University Health Sciences Animal Care and Use Committee and conducted under an approved protocol. Briefly, the tibialis anterior and soleus muscles of the hind limbs were dissected and then enzymatically digested to obtain the MPCs. Cells were washed with myogenic media (high glucose DMEM, 20% FBS, 10% Horse Serum, 1% chick embryo extract, antibiotics) and cultured for 3 days. The media was replaced with seeding media (low glucose DMEM, 15% FBS, antibiotics) and cells were expanded until adequate numbers were obtained. Although the culture was not assessed for fibroblasts, this technique has been previously reported by our collaborators [12], and these previous studies have shown that the use of myogenic media achieves cell populations that are positive for muscle-specific markers including myo-D, desmin, and myosin. We note that these primary cells were not expanded by multiple passages in culture, but were passaged only one time for loading into keratin hydrogels (see section 2.7, below).

2.7. Myoblast progenitor cell incorporation into keratin hydrogels and determination of cell viability

After 7 total days in culture, MPCs were removed from culture by EDTA/trypsin, and the trypsin was deactivated by one wash with seeding media (described above). Cells were resuspended at 250,000 cells/mL in seeding media without serum and added to KOS powder, which was then allowed to spontaneously gel at 37 °C for 2 hours. The gel was dispensed into a 24-well tissue culture plate and covered with seeding media. Viable cells within the hydrogel were determined daily by LavaCell® assay (Activ Motif, Carlsbad, CA) after 1, 2, or 4 days in culture with slight modifications to the manufacturer's recommendations to account for 3 dimensional staining challenges. Briefly, the myogenic culture media was removed and cells were washed twice in PBS. LavaCell was prepared at a concentration of 5μM, and 1mL was added to the well containing keratin hydrogel with cells. Cells were incubated for 30 minutes and then imaged immediately on a Leica DM4000 B microscope using a Texas Red filter in fluorescence mode. Images were collected with a Retiga 2000RV camera (Qimaging, Surrey, BC, Canada) coupled with ImagePro 6.2 software (Media Cybernetics, Inc., Bethesda, MD).

2.8. Subcutaneous implantation of keratin hydrogels

Keratin hydrogels loaded with MPCs and/or growth factors were prepared in a fashion similar to above for *in vitro* studies. The MPCs were trypsinized and resuspended at twice the desired concentration to achieve 250,000 cells per 100 μL hydrogel. A cocktail of the three growth factors above (IGF-1, bFGF, and VEGF) at twice their desired final concentration was added to the cell solution in equal volume to give the final desired growth factor concentration. This final mixture was added to the KOS powder to achieve a 12% weight:volume KOS hydrogel. The solution was allowed to spontaneously gel at 37 °C for 2 hours. We note that we consider these materials "flowable" hydrogels in that they are not rigid structures, but can still be injected via syringe.

All animal surgical procedures were conducted under aseptic conditions. C57BL/6J mice were weighed then anesthetized with a ketamine/xylazine cocktail (8 mg/kg Xylazine, 100 mg/kg Ketamine) given by intraperitoneal injection. The backs of the mice were shaved and washed with 70% ethanol and betadine. 4 pockets approximately 10mm in length in the longitudinal direction were made (2 on each side of the animal). A subcutaneous pocket was created by blunt dissection. The keratin hydrogels with or without cells and growth factor cocktails were injected into the implant site. Approximately 50μL of keratin hydrogel was added per pocket. The skin was then closed with nylon suture in a non-continuous pattern (~3–4 sutures per incision site). To avoid possible cross-contamination between the subcutaneous pockets, the same formulation was placed in each of the four pockets in each animal. While this decreases the randomization of the design, it was necessary to ensure proper interpretation of experimental results. A large number of cells were required for each implant; to minimize the number of animals used as donors, we also conducted surgeries in a non-randomized manner (e.g, all animals with keratose and MPCs were conducted together). This may further reduce the randomization of the design, but helped to reduce the number of donor animals required for these studies. Animals were allowed to recover from anesthesia and were given ketoprofen at 5 mg/kg immediately after surgery and for 3 days post-operatively. Mice were then housed for 1, 4, or 8 weeks post-operatively.

2.9. Gross evaluation and histological evaluation of explanted keratin hydrogels for vascularization and skeletal muscle phenotype

At the specified time points, mice were humanely euthanized with carbon dioxide gas and tissue at the site of the implant was initially investigated at the gross level for signs of tissue formation. The tissue was then explanted, placed in optimal cutting temperature compound (OCT, Ted Pella, Redding, CA), and snap frozen in liquid nitrogen. Samples were then stored at −80°C until sectioning on a Leica 1850 cryostat (Leica, Buffalo Grove, IL). 10 μm thick sections were collected on glass slides and stored at −20°C until staining. At the time of staining, sections were fixed with 10% neutral-buffered formalin for 1 minute.

Hematoxylin and eosin stains were conducted by standard techniques to observe any signs of inflammatory response and to determine basic phenotype of cells in and around the implant. Briefly, fixed sections on slides were stained with hematoxylin (1% w/v with alum, sodium iodate, and citric acid), washed repeatedly with water, stained with eosin working solution (1% w/v), washed again, exchanged through ethanol washes to xylenes, and coverslipped with Permount.

Immunohistochemical staining for vascularization was performed with a blood vessel staining kit (Millipore, Bellerica, MA), for von Willebrand factor using standard techniques. Briefly, after fixation, sections were blocked for 30 minutes, washed, and incubated with primary polyclonal antibody (rabbit anti-von Willebrand factor). Samples were incubated with primary antibody or with control (no primary antibody) for 2 hours in a humidified chamber. Sections were then rinsed three times and incubated for 1 hour with secondary antibody (biotinylated goat anti-rabbit) secondary in a humidified chamber. Sections were then rinsed three times and incubated with streptavidin-alkaline phosphatase in a humidified chamber. Sections were then washed and incubated with chromogen until color change was

observed (~ 2 minutes). Sections were then washed, dehydrated through xylenes, and coverslipped with Permount. Staining methods for desmin were similar with the exception that an Impress anti-goat secondary (Vector Labs) was used for visualization. Sections were imaged as described above for H&E stains.

2.10. Statistical analysis

Quantitative results were analyzed by one-way ANOVA followed by Tukey's post-hoc analysis in Minitab 14 unless otherwise noted. Values of $P < 0.05$ were taken to be statistically significant. Number of samples and representation of error bars (standard deviation or standard error of the mean) are shown in the figures as appropriate.

3. Results

3.1. Human skeletal muscle myoblast (hSMM) response to keratin

In order to assess the potential of using keratin as an alternative to widely used natural polymers such as collagen, the response of hSMMs to keratin was characterized. Thin keratin coatings were applied to uncoated tissue culture-treated polystyrene or tissue culture polystyrene coated with KOS (alpha or gamma fractions), KTN (alpha or gamma fractions), Matrigel, or collagen. Giemsa staining (Figure 2) shows that hSMMs displayed typical morphology characterized by spreading and preliminary myotube formation when cultured for two weeks on all of the coatings. However the keratin coatings (particularly alpha KOS and alpha KTN) led to more ordered structures with no aberrant morphology. Data shown in Figure 2 shows that both KOS and KTN coatings (alpha or gamma fractions) led to statistically significant increases in the number of multinucleated and mature cells, compared to the more traditional coatings. The one exception was gamma-KTN that was not significantly different than collagen or Matrigel™. Under these non-differentiating conditions, hSMMs remained viable and showed expected morphology.

Cell proliferation and adhesion were also assessed by using hSMM in culture. hSMM were plated on cell culture dishes containing the four different keratin coatings as well as collagen, Matrigel™, or uncoated controls. After 1 hour, adhesion following four washes was measured on cells compared to unwashed control cells (Figure 3A). The results show that all four keratin fractions and Matrigel™ provided similar levels of adhesion for hSMM, compared with collagen and the uncoated controls. The only statistically significant difference in adhesion was that gamma KOS led to greater levels of adhesion than collagen. Proliferation over the course of six days did not differ significantly between the substrates used (Figure 3B). These data demonstrate that keratin is comparable to other cell culture coatings in supporting hSMM adherence and proliferation.

3.2. Rheological characterization of keratin hydrogels

Rheology was used to assess various formulations of keratin gels for growth factor and cellular delivery. Figure 4 shows results of plate-plate frequency sweep rheological tests for three-dimensional keratin hydrogels fabricated from KOS or KTN. Results shown are from a single representative experiment. Direct comparisons between KOS and KTN were assessed by using various percent concentrations (measured weight to volume). 20% (w/v) KOS and

KTN gels were formed as above and subjected to rheological testing. Figures 4A and 4B shows that 20% KOS and KTN hydrogels have similar G′ (elastic modulus) values but that 20% KTN has a G″ (viscous modulus) that is approximately an order of magnitude less than 20% KOS. This is summarized by the tan δ (which is G″/G′ or a ratio of viscous to elastic moduli) for 20% KTN which is an order of magnitude less and reflects that KTN is relatively more elastic or less viscous due to the presence of the covalent disulfide cross-links.

The moduli for 20% KOS and KTN gels were both considered too high for cell incorporation, and both gels were relatively rigid. Therefore, gels were fabricated with elastic moduli closer to 100 Pa; a value that typically provide gels with a more flowable nature. Figures 4C and 4D shows that 12% (w/v) KOS and 8% (w/v) KTN hydrogels had elastic moduli closer to 100 Pa, which is a range where gels display a more flowable nature (note the scale change between Figure 4A–B and Figure 4C–D). These formulations were therefore selected for *in vitro* and *in vivo* testing with MPCs. Note the difference in scales between the 20% gels.

3.3. Release of growth factors from keratose and kerateine hydrogels

To determine the ability to modulate the amount of growth factor delivered, *in vitro* release studies were conducted by loading KOS or KTN hydrogels with three different growth factors known to play roles in the differentiation and viability of muscle progenitor cells: IGF-1, bFGF, and VEGF. VEGF has a well-known role in promoting angiogenesis, which has been shown to increase the long-term viability of engineered skeletal muscle [54]. bFGF plays a known role in wound healing and repair of many tissues including skeletal muscle [55] and may help to overcome poor healing [56] associated with its down-regulation following injury [57]. IGF-1 plays a key role in cell recruitment to improve muscle mass and hypertrophy [58–60].

The amount of released growth factor was determined by measuring the eluted growth factor by using an ELISA. The amount of keratin degraded from the gels into the PBS was determined by a modified Lowry assay. In Figures 5A and 5B, the ■ shows the percentage of degradation of KOS and KTN, respectively, based on the initial keratin weight in the hydrogels. Note that the y-axes on Figures 5A and 5B are very different, reflecting that the KTN gels degrade more slowly than the KOS gels. The inset to Figure 5B shows the KTN on the same scale as KOS in Figure 5A to better highlight the difference in scales of keratin degradation and growth factor release for KTN versus KOS. Figures 5A and 5B also show the percentage of each growth factor released (based on the initial loading amount) for both KOS and KTN. It can be seen that total keratin degraded from the KOS and KTN gels differs by approximately 5-fold (compare Figure 5A and 5B). This is consistent with previous results [50,51] and the hypothesis that KOS degrades more rapidly than KTN due to presence of covalent disulfide bonds within KTN. Release of all growth factors correlates strongly with keratin degradation, but there are clear differences in the percent release of each growth factor. For both KOS and KTN, bFGF showed the most rapid release, with the total release of bFGF exceeding the amount of degraded keratin (both KOS and KTN). VEGF showed nearly 40-fold lower levels of release than bFGF in both KOS and KTN gels

and the total percent release was less than the amount of degraded keratin. Of the growth factors tested, IGF-1 was the only growth factor to show a different pattern of release. The release profiles from KOS, corresponded to the observed degradation of KOS, whereas there was little release observed from KTN, which corresponds to its slower degradation profile. We have also recently conducted a separate equilibrium binding study (results not shown) in which we observed that IGF-1 binds with higher affinity to KTN than to KOS. Thus, the results observed in this study may be related to the properties of the keratin hydrogel materials (KTN vs. KOS) as well as the physiochemical properties of the drug or growth factor (in this case, IGF-1).

Despite differences in absolute amounts of release, release for each growth factor was characterized by an initial weak burst release followed by eventual plateau, consistent with first order release kinetics.

3.4. MPC viability in keratin hydrogels

A key objective of these studies was to encapsulate MPCs in keratin hydrogels for *in vivo* delivery. It was therefore necessary to develop modifications to the formation of the hydrogels to allow incorporation of cells. Gelation of KTN was found to optimally occur with water as the hydrating solution, preventing the use of KTN for further evaluation of cell viability in three-dimensional hydrogels *in vitro* or *in vivo* due to the presence of salts in cell culture media. In addition, MPCs placed in PBS before addition to KOS powder did not remain viable (data not shown). Therefore cells were maintained in seeding media when added to KOS powders to form hydrogels. The presence of viable MPCs in KOS gels was determined by LavaCell. As shown in Figure 6, the presence of viable MPCs in KOS hydrogels could be observed over the over the course of 96 hours. While it is possible that cell death occurred over the course of these 96 hours, our interpretation is that the levels of live cells in the keratose hydrogels remained consistent with the levels on tissue culture polystyrene. To insure minimal cell losses or phenotypic changes prior to implantation, MPCs in KOS were implanted 2 hours after gelation.

3.5. Histological evaluation of explanted keratose hydrogels

KOS hydrogels containing a growth factor cocktail of IGF-1, bFGF, and VEGF (at the concentrations described above for each individually) and MPCs were implanted in a mouse subcutaneous model to assess tissue formation resulting from the implanted keratin/cell/growth factor mixture. KOS hydrogels were explanted at various time points from 1 – 8 weeks. Figure 7 shows representative H&E images from KOS scaffolds only, KOS scaffolds loaded with MPCs, and KOS scaffolds loaded with MPCs and a growth factor cocktail at 1, 4, and 8 weeks post-implant. Histological assessment showed that implantation did not produce significant signs of inflammation such as multi-nucleated macrophages. In particular, if a significant immune response were observed, it would be expected to occur near the periphery of the KOS implants (examples of which are shown by white arrows), which was not observed (Figure 7). Cells observed within the scaffolds had morphology consistent of MPCs and vascular formation was seen within the constructs (Figure 7, black arrow).

3.6. Gross and immunohistochemical observation of vascular formation

The H&E images indicated that KOS gels (with or without cells and growth factors) had incorporated into the host animal with minimal inflammatory response. The growth factor cocktail formulation contained VEGF to promote vascular formation and the opportunity for long-term cell viability. As noted above, H&E images showed signs of vascular structures (Figure 7, black arrow). Gross imaging of the subcutaneous area (Figure 8A) after humane euthanization clearly shows the presence of large vascular networks at 1 week, though decreasing levels of vasculature were observed at 4 and 8 weeks (not shown). This vascularization was only seen in groups that contained VEGF and was not present in the keratin only or keratin plus cell groups (Figure 8A). Staining for von Willebrand factor shows the presence of endothelial cells, confirming interpretation of H&E results and the gross examination. These results indicate that the VEGF delivered from KOS hydrogels remained bioactive *in vivo* and that keratin alone or keratin plus MPCs is not sufficient to induce vascularization.

3.7. Immunohistochemical evaluation of muscle cell development

The H&E images indicated that KOS hydrogels (indicated by white arrows as in Figure 7) with incorporated cells had morphology consistent with MPCs (Figure 9). While KOS gels only (Figure 9A) did not show desmin-positive cells, the 4 week time points for KOS gels that contained MPCs (Figure 9 C) did show desmin staining (black arrows), which suggests the presence of myogenic cells. KOS with MPCs did not show desmin staining at the 1 and 8 week time point in our sections (Figure 9B and D). Lack of staining at the 8 week time point may be due to the degradation of KOS over this time period.

4. Discussion

In these studies, we sought to exploit our previous observations that rate of keratin degradation could be used to control the rate therapeutic agent release [36,52] while also providing a system for cellular delivery. This combination would provide the materials (i.e., keratin), signals (i.e., growth factors), and cellular components of the tissue engineering triad that will likely be necessary to ultimately promote healing of VML injuries. We specifically evaluated both material properties of keratin (rheology, degradation, and growth factor release) and the biological response to these materials (cell morphology, proliferation, and viability as well as *in vivo* performance) to investigate the suitability of keratin hydrogels as material for VML.

The initial approach of these studies was to investigate the cellular response to keratin materials as 2-D coatings. Interestingly, the keratin coatings supported the striated morphology expected of hSMM cells in culture, with Giemsa staining indicating the best organization on the alpha fractions of keratose and kerateine. These qualitative assessments were supported by an analysis of the number of multi-nucleated cells, which is an indicator of myoblast maturation. Again, the keratin fractions and in particular alpha KOS, alpha KTN, and gamma KOS supported multi-nucleated cells as well or better than Matrigel™, collagen, or uncoated TCPS. The keratin coatings also supported levels of cell adhesion comparable to Matrigel™ and greater than collagen or uncoated TCPS, though differences in

adhesion were not found to be statistically significant. Similarly, keratin coatings led to similar rates of hSMM proliferation indicating that any increases in cell adhesion did not reduce the rate of proliferation and suggesting that these materials could support cell growth at levels comparable to more commonly used coatings such as Matrigel™ or collagen.

We note that a pilot gene array experiment was conducted on gamma-KOS (in comparison to untreated TCPS, collagen, and Matrigel™) because this was the only keratin fraction to lead to significant changes in cell adhesion (see Figure 3). The methods and results are presented as Supplemental Material because only one form of keratin was tested for this gene array experiment and, ultimately, this component (gamma-KOS) was not included in the hydrogel formulations tested in vivo. Nonetheless, given the similarities between the keratin fractions in terms of proliferation and adhesion, this study provides possible insight into the effects of keratin biomaterials on hSMM cells. The gene array data (Supplemental Figure 1) showed that after as many as ten days in culture, gamma-KOS had minimal impacts on cellular gene expression profiles and that cells grown on gamma-KOS and collagen had more similar gene expression profiles to each other and to cells grown on uncoated plates than to cells grown on the undefined Matrigel™ matrix. This might be expected as Matrigel is composed of multiple structural proteins and growth factors.

Although the two-dimensional data indicated that keratin was supportive of myoblasts, 2-dimensional systems cannot be used as cell and growth factor carriers. We therefore sought to study the characteristics of three-dimensional keratin hydrogels as carriers, and more specifically, to investigate the utility of KOS versus KTN as the carrier system. In order to do this, gels were formed with 100% alpha fractions of keratin (no gamma) to examine the contribution of the higher molecular weight alpha keratin that has been hypothesized to be responsible for gel polymerization by chain entanglement. Results of the rheological studies confirmed previous results and theory related to gels formed from the two modes of extraction. In particular, we note that the tan δ value of KTN gels was an order of magnitude lower than KOS gels when gels were at the same weight percent (20%). This suggests that the presence of the disulfide cross-links in KTN lead to a relative increase in elastic nature of the material, as expected. Although not surprising, it is also clear that the elastic and viscous moduli are highly dependent on the weight percent, with keratin hydrogels of about ½ the concentration described above (8% for KOS and 12% for KTN) having two-three orders of magnitude reduction in the moduli. A key result of these rheological studies, however, is that the materials exhibit characteristics associated with gel formation [61,62]. The rheological studies also aided in selection of the gel formulations used in subsequent release, cell, and *in vivo* studies with 3-D hydrogels. In particular, it is noted that the selected formulations were flowable and, for *in vivo* studies (see below), were able to be injected via a syringe into the tissue pockets. This could ultimately be important for some types of injuries where injectable tissue-promoting materials are necessary.

The presence of disulfide cross-links in the KTN hydrogels (or lack thereof in KOS hydrogels) has important implications not only for the material's mechanical properties, but also for its degradation and growth factor release profiles. The data shown here suggests that the presence of disulfide bonds in KTN leads to a slower degradation than keratose hydrogels lacking the cross-links. This is significant because we have previously

reported [36,63] and have observed here (Figure 5), that delivery of therapeutic agents is highly correlated to the degradation of the keratin hydrogels *in vitro*. This is particularly interesting given that one challenge with many natural protein-based materials such as collagen, is that although they support cell attachment and proliferation, they are typically not suited for controlled degradation or growth factor release without the introduction of external crosslinkers. The order-of-magnitude differences for both degradation rate and growth factor release between KTN and KOS (see Figure 5), shows the inherent flexibility that keratins have through the presence of their disulfide bonds. This result is significant in that keratin represents a naturally-derived polymer system that can be formulated to have either slow (KTN) or more rapid (KOS) degradation and delivery for growth factor delivery. We have also observed (data not shown) that modulation of the gel weight percentages and the ratio of alpha to gamma sub-fractions can also be used to achieve more control over degradation and growth factor release. Lastly, in addition to the structural properties of keratin that control the rate of release, the physiochemical properties of the growth factor molecules also play a role. This is most readily noticed in the differences in release rates between bFGF, IGF-1 and VEGF in which similar keratin compositions showed markedly different release profiles. We suspect that these differences in release rates are due to differences in both molecular weight and isoelectric points of the growth factors themselves. We note that some growth factors associate with a higher non-covalent binding affinity to keratin than others. In the case of IGF-1, this equilibrium binding affinity is higher for KTN than for KOS (data not shown), which would also explain the release profiles shown in Figure 5. It is also worth noting, however, that the growth factor release profiles were determined by ELISA. Given the low release percentages of some growth factors, particularly IGF-1 and VEGF from KTN, we cannot rule out the possibility that the growth factors lost bioactivity, leading to the loss of detectability by the ELISA.

Growth factor delivery has come to the forefront of clinical practice with the use of Medtronic's Infuse system for rhBMP-2 delivery in bone regeneration, making the results of the controlled growth factor release from keratin interesting. However, a single growth factor with the efficacy of rhBMP-2 is yet to be identified for volumetric muscle loss injuries. This suggests, at least for the foreseeable future, that a combination of growth factors and cells will be required to promote tissue engineering-based repair of these injuries. We, therefore, investigated the ability of keratin hydrogels to deliver both cells and a cocktail of growth factors. We have observed that although KTN can be formed into hydrogels by using water, it is not capable of forming gel in the presence of sodium chloride [64]. Thus, while KTN may have use as a cell-free growth factor delivery system, we were unable to use KTN extracts as a cell delivery system due to the sodium chloride present in cell media. However, KOS constructs are not sensitive to salt concentrations, and thus were used for both cell delivery and growth factor delivery in these studies. Cell viability studies showed that mouse MPCs loaded into keratin hydrogels maintained viability over the course of four days (Figure 6). Unfortunately, the anionic nature of keratin at neutral pH prevented investigation of the presence of dead cells in the gels. Therefore, for *in vivo* implantation of the KOS/growth factor/MPC constructs, we implanted the constructs immediately after gelation to minimize any possible loss of cell viability during *in vitro* gelation.

We then investigated the behavior of these KOS/growth factor/MPC constructs *in vivo*, noting that constructs were immediately implanted after gelation and cells did not need to survive for 4 days *in vitro*, although they can survive this long if necessary (as shown in Figure 6). As noted above, these constructs were flowable and injectable, and were implanted via injection through a syringe. Our *in vivo* results illustrate two important points. First, it is clear that the growth factors (or least some of them) remain bioactive. This is evidenced by the obvious formation (verified at the microscopic level by histology) of vascular structures. Both IGF-1 and VEGF are capable of achieving vascularization, though it seems likely that the VEGF was responsible for the observed vascularization of the constructs. Thus the gelation process and *in vivo* incubation does not appear to deactivate the growth factors. Secondly, the implanted cells remained viable and led to the formation of primitive muscle structures. This is evidenced by the desmin staining in animals treated with the KOS/growth factor/MPC formulations at the 4 week time point compared to KOS only, which did not show desmin positive cells. The tissue formation shown in H&E images indicates the formation of very primitive muscle tissue, likely due to the presence of the injected cells. We note that at the 8 week time point (Figure 9D), desmin staining was not observed. This corresponds to the degradation or resorption of the KOS by this time point as indicated by the H&E staining in Figure 7. Our interpretation of this result is that the delivered cells are capable of forming a primitive muscle-like construct, but that the material "scaffold" degraded too rapidly to allow for full and sustainable tissue formation. In on-going work, we are developing approaches to enhance the longevity of the keratin gels (with cells) in order to sustain and mature these muscle-like constructs.

There are several considerations related to the current study that should be noted in terms of potential clinical translation of this technology. One consideration is the use of keratin itself. The patent-pending, proprietary extraction system used for the keratins extracted for this system achieves approximately 60% recovery (by mass) of the starting material as keratin protein with low batch-to-batch variability. In terms of availability of raw material (i.e., hair), the hair is sourced from the Chinese wig industry, making it a "renewable" source. Given the recoveries noted above, the amount of raw material is sufficient for virtually any manufacturing requirements.

A second consideration related to this study is that formation (or regeneration) of functional skeletal muscle was not achieved in the subcutaneous *in vivo* model. Indeed, the primary objective of this study was to assess the ability to deliver cells capable of muscle formation in a keratin system and to assess the effects of the growth factor cocktail. In order to assess the ability of this system to achieve functional skeletal muscle formation, our team is currently investigating the performance of similar keratin-based constructs in a mouse Latissimus dorsi VML model as well as a rat tibialis anterior VML model. Challenges associated with these models compared to the subcutaneous model used in the current study include lack of vascularization (which could lead to cell death) and the rate of innervation of the constructs leading to atrophy of any muscle tissue formed/regenerated.

A third consideration for the current system is the use of growth factors. Despite the functional potential of growth factors such as rhBMP-2 and those used in the studies reported in this manuscript, regulatory approval of such therapies is challenging. The

complications associated with rhBMP-2 including ectopic bone growth and concerns over tumor formation [65] have heighted awareness regarding the use of growth factors for regenerative medicine applications. In addition, as noted above, a single growth factor for muscle regeneration that would be similar to rhBMP-2 for bone regeneration is not known. Further, constructs such as the one described in this report which contain cells would be considered combination products with components that may be classified as drugs, devices, and biologics. Future studies that would allow the system described in this report to use a single growth factor (either an existing molecule or one yet to be discovered) instead of the cocktail of growth factors used here could be advantageous in considering regulatory approval.

Despite these limitations, the results of the studies in this report do show that the constructs integrated into the host tissue with minimal inflammatory response. This is a generally important characteristic for materials used in TERM strategies, and in particular for cell delivery strategies in general to avoid effects of inflammatory response on implanted (delivered) cells. Further, this natural polymer was able to support both cell and growth factor delivery within the context of a flowable and injectable system. Given that *in vitro* data from these studies showed that keratin supported a robust skeletal muscle phenotype compared with collagen or Matrigel™, further studies with keratin for skeletal muscle tissue formation are warranted. In particular, it will be necessary and important in the future to identify which growth factors were primarily responsible for vascularization and cell phenotype in order to simplify the constructs.

5. Conclusions

This study demonstrates the suitability of keratin biomaterials as cell and growth factor carrier systems as indicated by their ability to support skeletal muscle phenotype in both 2 and 3-dimensional culture systems. The 3-dimensional hydrogel system is capable of providing tunable delivery of growth factors from a natural polymer system matrix. This system is compatible with repair strategies for volumetric muscle loss with flowable materials that can integrate into the host with minimal inflammatory response. These studies also suggest that these materials could be used for tissue engineering repair strategies in other injury models that require materials, growth factors, and cells.

Supplementary Material

Refer to Web version on PubMed Central for supplementary material.

Acknowledgments

This work was funded by the U.S. Department of Defense/U.S. Army SBIR/STTR Program by contract numbers W81XWH-11-C-0060 (Phase I SBIR to ST) and W81XWH-10-C-065 (Phase I SBIR to EPK). The study was also supported in part by the National Institutes of Health grant R01AR061391 (JMS), but the content of this article is solely the responsibility of the authors and does not necessarily represent the official views of the National Institutes of Health or the Department of Defense. The authors thank Dr. George Christ and Ms. Ashley Dannahower for assistance with isolation and culture of muscle progenitor cells, Ms. Cathy Mathis for assistance with histology, and Ms. Afton Vechery for assistance with hSMM culture.

References

1. Atala A, Bauer SB, Soker S, Yoo JJ, Retik AB. Tissue-engineered autologous bladders for patients needing cystoplasty. Lancet. 2006; 367(9518):1241–6. [PubMed: 16631879]
2. Macchiarini P, Jungebluth P, Go T, Asnaghi MA, Rees LE, Cogan TA, Dodson A, Martorell J, Bellini S, Parnigotto PP, et al. Clinical transplantation of a tissue-engineered airway. Lancet. 2008; 372(9655):2023–30. [PubMed: 19022496]
3. McKay WF, Peckham SM, Badura JM. A comprehensive clinical review of recombinant human bone morphogenetic protein-2 (INFUSE Bone Graft). Int Orthop. 2007; 31(6):729–34. [PubMed: 17639384]
4. Fagerholm P, Lagali NS, Ong JA, Merrett K, Jackson WB, Polarek JW, Suuronen EJ, Liu Y, Brunette I, Griffith M. Stable corneal regeneration four years after implantation of a cell-free recombinant human collagen scaffold. Biomaterials. 2014; 35(8):2420–7. [PubMed: 24374070]
5. Matsumura G, Miyagawa-Tomita S, Shin'oka T, Ikada Y, Kurosawa H. First evidence that bone marrow cells contribute to the construction of tissue-engineered vascular autografts in vivo. Circulation. 2003; 108(14):1729–34. [PubMed: 12963635]
6. Sharma B, Fermanian S, Gibson M, Unterman S, Herzka DA, Cascio B, Coburn J, Hui AY, Marcus N, Gold GE, et al. Human cartilage repair with a photoreactive adhesive-hydrogel composite. Science translational medicine. 2013; 5(167):167ra6.
7. Waterman BR, Schoenfeld AJ, Holland CA, Goodman GP, Belmont PJ Jr. Burden of musculoskeletal disease and nonbattle nontraumatic injury in both war and disaster zones. Journal of surgical orthopaedic advances. 2011; 20(1):23–9. [PubMed: 21477529]
8. Burden of musculoskeletal disease overview. The burden of musculoskeletal diseases in the United States: prevalence, societal and economic cost. 2011:1–20.
9. Burden of musculoskeletal disease: Injuries. 2011:129–179.
10. Mase VJ Jr, Hsu JR, Wolf SE, Wenke JC, Baer DG, Owens J, Badylak SF, Walters TJ. Clinical application of an acellular biologic scaffold for surgical repair of a large, traumatic quadriceps femoris muscle defect. Orthopedics. 2010; 33(7):511. [PubMed: 20608620]
11. Corona BT, Garg K, Ward CL, McDaniel JS, Walters TJ, Rathbone CR. Autologous minced muscle grafts: a tissue engineering therapy for the volumetric loss of skeletal muscle. Am J Physiol Cell Physiol. 2013; 305(7):C761–75. [PubMed: 23885064]
12. Machingal MA, Corona BT, Walters TJ, Kesireddy V, Koval CN, Dannahower A, Zhao W, Yoo JJ, Christ GJ. A tissue-engineered muscle repair construct for functional Keratin hydrogel carrier system 31 restoration of an irrecoverable muscle injury in a murine model. Tissue engineering Part A. 2011; 17(17–18):2291–303. [PubMed: 21548710]
13. Tamada Y, Ikada Y. Fibroblast growth on polymer surfaces and biosynthesis of collagen. Journal of biomedical materials research. 1994; 28(7):783–9. [PubMed: 8083246]
14. Delaittre G, Greiner AM, Pauloehrl T, Bastmeyer M, Barner-Kowollik C. Chemical approaches to synthetic polymer surface biofunctionalization for targeted cell adhesion using small binding motifs. Soft Matter. 2012; 8(28):7323–7347.
15. Mariner PD, Wudel JM, Miller DE, Genova EE, Streubel SO, Anseth KS. Synthetic hydrogel scaffold is an effective vehicle for delivery of INFUSE (rhBMP2) to critical-sized calvaria bone defects in rats. Journal of orthopaedic research: official publication of the Orthopaedic Research Society. 2013; 31(3):401–6. [PubMed: 23070779]
16. Khetan S, Guvendiren M, Legant WR, Cohen DM, Chen CS, Burdick JA. Degradation-mediated cellular traction directs stem cell fate in covalently crosslinked three-dimensional hydrogels. Nature materials. 2013; 12(5):458–65. [PubMed: 23524375]
17. Singh A, Zhan JA, Ye ZY, Elisseeff JH. Modular Multifunctional Poly(ethylene glycol) Hydrogels for Stem Cell Differentiation. Advanced Functional Materials. 2013; 23(5):575–582.
18. Kolb CM, Pierce LM, Roofe SB. Biocompatibility comparison of novel soft tissue implants vs commonly used biomaterials in a pig model. Otolaryngology--head and neck surgery: official journal of American Academy of Otolaryngology-Head and Neck Surgery. 2012; 147(3):456–61. [PubMed: 22687327]

19. Bostman OM. Intense granulomatous inflammatory lesions associated with absorbable internal fixation devices made of polyglycolide in ankle fractures. Clinical orthopaedics and related research. 1992; (278):193–9.
20. Taylor MS, Daniels AU, Andriano KP, Heller J. Six bioabsorbable polymers: in vitro acute toxicity of accumulated degradation products. Journal of applied biomaterials: an official journal of the Society for Biomaterials. 1994; 5(2):151–7. [PubMed: 10147175]
21. Rowley JA, Mooney DJ. Alginate type and RGD density control myoblast phenotype. Journal of biomedical materials research. 2002; 60(2):217–23. [PubMed: 11857427]
22. Jeong SI, Jeon O, Krebs MD, Hill MC, Alsberg E. Biodegradable photo-crosslinked alginate nanofibre scaffolds with tuneable physical properties, cell adhesivity and growth factor release. European cells & materials. 2012; 24:331–43. [PubMed: 23070945]
23. Heino J. The collagen family members as cell adhesion proteins. Bioessays. 2007; 29(10):1001–1010. [PubMed: 17876790]
24. Aumailley M, Timpl R. Attachment of cells to basement membrane collagen type IV. The Journal of cell biology. 1986; 103(4):1569–75. [PubMed: 3771647]
25. Zeeman R, Dijkstra PJ, van Wachem PB, van Luyn MJ, Hendriks M, Cahalan PT, Feijen J. Successive epoxy and carbodiimide cross-linking of dermal sheep collagen. Biomaterials. 1999; 20(10):921–31. [PubMed: 10353646]
26. Wang Y, Zhang L, Hu M, Wen W, Xiao H, Niu Y. Effect of chondroitin sulfate modification on rhBMP-2 release kinetics from collagen delivery system. J Biomed Mater Res A. 2010; 92(2):693–701. Keratin hydrogel carrier system 33. [PubMed: 19263491]
27. Parenteau-Bareil R, Gauvin R, Cliche S, Gariepy C, Germain L, Berthod F. Comparative study of bovine, porcine and avian collagens for the production of a tissue engineered dermis. Acta biomaterialia. 2011; 7(10):3757–65. [PubMed: 21723967]
28. Friess W. Collagen--biomaterial for drug delivery. European journal of pharmaceutics and biopharmaceutics: official journal of Arbeitsgemeinschaft fur Pharmazeutische Verfahrenstechnik e V. 1998; 45(2):113–36. [PubMed: 9704909]
29. Lin YC, Ramadan M, Hronik-Tupaj M, Kaplan DL, Philips BJ, Sivak W, Rubin JP, Marra KG. Spatially controlled delivery of neurotrophic factors in silk fibroin-based nerve conduits for peripheral nerve repair. Ann Plast Surg. 2011; 67(2):147–55. [PubMed: 21712696]
30. Linnes MP, Ratner BD, Giachelli CM. A fibrinogen-based precision microporous scaffold for tissue engineering. Biomaterials. 2007; 28(35):5298–306. [PubMed: 17765302]
31. Daamen WF, Veerkamp JH, van Hest JC, van Kuppevelt TH. Elastin as a biomaterial for tissue engineering. Biomaterials. 2007; 28(30):4378–98. [PubMed: 17631957]
32. Chien KB, Aguado BA, Bryce PJ, Shah RN. In vivo acute and humoral response to three-dimensional porous soy protein scaffolds. Acta Biomater. 2013; 9(11):8983–90. [PubMed: 23851173]
33. Tachibana A, Furuta Y, Takeshima H, Tanabe T, Yamauchi K. Fabrication of wool keratin sponge scaffolds for long-term cell cultivation. J Biotechnol. 2002; 93(2):165–70. [PubMed: 11738723]
34. Richter JR, de Guzman RC, Van Dyke ME. Mechanisms of hepatocyte attachment to keratin biomaterials. Biomaterials. 2011; 32(30):7555–61. [PubMed: 21782237]
35. Kowalczewski CJ, Tombyln S, Wasnick DC, Hughes MR, Ellenburg MD, Callahan MF, Smith TL, Van Dyke ME, Burnett LR, Saul JM. Reduction of ectopic bone growth in Keratin hydrogel carrier system 34 critically-sized rat mandible defects by delivery of rhBMP-2 from kerateine biomaterials. Biomaterials. 2014; 35(10):3220–8. [PubMed: 24439399]
36. Saul JM, Ellenburg MD, de Guzman RC, Van Dyke M. Keratin hydrogels support the sustained release of bioactive ciprofloxacin. Journal of biomedical materials research Part A. 2011; 98(4): 544–53. [PubMed: 21681948]
37. Sierpinski P, Garrett J, Ma J, Apel P, Klorig D, Smith T, Koman LA, Atala A, Van Dyke M. The use of keratin biomaterials derived from human hair for the promotion of rapid regeneration of peripheral nerves. Biomaterials. 2008; 29(1):118–28. [PubMed: 17919720]
38. Apel PJ, Garrett JP, Sierpinski P, Ma J, Atala A, Smith TL, Koman LA, Van Dyke ME. Peripheral nerve regeneration using a keratin-based scaffold: long-term functional and histological outcomes in a mouse model. The Journal of hand surgery. 2008; 33(9):1541–7. [PubMed: 18984336]

39. Lin YC, Ramadan M, Van Dyke M, Kokai LE, Philips BJ, Rubin JP, Marra KG. Keratin gel filler for peripheral nerve repair in a rodent sciatic nerve injury model. Plastic and reconstructive surgery. 2012; 129(1):67–78. [PubMed: 22186500]
40. Hill PS, Apel PJ, Barnwell J, Smith T, Koman LA, Atala A, Van Dyke M. Repair of peripheral nerve defects in rabbits using keratin hydrogel scaffolds. Tissue engineering Part A. 2011; 17(11–12):1499–505. [PubMed: 21275820]
41. Dias GJ, Peplow PV, McLaughlin A, Teixeira F, Kelly RJ. Biocompatibility and osseointegration of reconstituted keratin in an ovine model. J Biomed Mater Res A. 2010; 92(2):513–20. Keratin hydrogel carrier system 35. [PubMed: 19213058]
42. Thilagar S, Jothi NA, Omar AR, Kamaruddin MY, Ganabadi S. Effect of keratin-gelatin and bFGF-gelatin composite film as a sandwich layer for full-thickness skin mesh graft in experimental dogs. J Biomed Mater Res B Appl Biomater. 2009; 88(1):12–6. [PubMed: 18161832]
43. Shen D, Wang X, Zhang L, Zhao X, Li J, Cheng K, Zhang J. The amelioration of cardiac dysfunction after myocardial infarction by the injection of keratin biomaterials derived from human hair. Biomaterials. 2011; 32(35):9290–9. [PubMed: 21885119]
44. Cardamone JM, Nunez A, Garcia RA, Aldema-Ramos M. Characterizing Wool Keratin. Research Letters in Materials Science. 2009; 2009:1–5.
45. Katoh K, Shibayama M, Tanabe T, Yamauchi K. Preparation and physicochemical properties of compression-molded keratin films. Biomaterials. 2004; 25(12):2265–72. [PubMed: 14741591]
46. Reddy N, Jiang Q, Jin E, Shi Z, Hou X, Yang Y. Bio-thermoplastics from grafted chicken feathers for potential biomedical applications. Colloids and surfaces B, Biointerfaces. 2013; 110C:51–58.
47. Rouse JG, Van Dyke ME. A review of keratin-based biomaterials for biomedical applications. Materials. 2010; 3(2):999–1014.
48. Reichl S. Films based on human hair keratin as substrates for cell culture and tissue engineering. Biomaterials. 2009; 30(36):6854–6866. [PubMed: 19783297]
49. Crewther WG, Fraser RD, Lennox FG, Lindley H. The chemistry of keratins. Adv Protein Chem. 1965; 20:191–346. [PubMed: 5334826]
50. de Guzman RC, Merrill MR, Richter JR, Hamzi RI, Greengauz-Roberts OK, Van Dyke ME. Mechanical and biological properties of keratose biomaterials. Biomaterials. 2011; 32(32):8205–17. [PubMed: 21835462]
51. Hill P, Brantley H, Van Dyke M. Some properties of keratin biomaterials: kerateines. Biomaterials. 2010; 31(4):585–93. [PubMed: 19822360]
52. de Guzman RC, Saul JM, Ellenburg MD, Merrill MR, Coan HB, Smith TL, Van Dyke ME. Bone regeneration with BMP-2 delivered from keratose scaffolds. Biomaterials. 2013; 34(6):1644–56. [PubMed: 23211447]
53. Corona BT, Machingal MA, Criswell T, Vadhavkar M, Dannahower AC, Bergman C, Zhao W, Christ GJ. Further development of a tissue engineered muscle repair construct in vitro for enhanced functional recovery following implantation in vivo in a murine model of volumetric muscle loss injury. Tissue engineering Part A. 2012; 18(11–12):1213–28. [PubMed: 22439962]
54. Germani A, Di Carlo A, Mangoni A, Straino S, Giacinti C, Turrini P, Biglioli P, Capogrossi MC. Vascular endothelial growth factor modulates skeletal myoblast function. The American journal of pathology. 2003; 163(4):1417–28. [PubMed: 14507649]
55. Anderson JE, Mitchell CM, McGeachie JK, Grounds MD. The time course of basic fibroblast growth factor expression in crush-injured skeletal muscles of SJL/J and BALB/c mice. Experimental cell research. 1995; 216(2):325–34. [PubMed: 7843277]
56. Dubay DA, Wang X, Kuhn MA, Robson MC, Franz MG. The prevention of incisional hernia formation using a delayed-release polymer of basic fibroblast growth factor. Annals of surgery. 2004; 240(1):179–86. [PubMed: 15213634]
57. Fu X, Cuevas P, Gimenez-Gallego G, Tian H, Sheng Z. Ischemia and reperfusion reduce the endogenous basic fibroblast growth factor (bF GF) in rat skeletal muscles. Chinese medical journal. 1995; 108(9):699–703. [PubMed: 8575238]
58. Barton-Davis ER, Shoturma DI, Musaro A, Rosenthal N, Sweeney HL. Viral mediated expression of insulin-like growth factor I blocks the aging-related loss of skeletal muscle function.

Proceedings of the National Academy of Sciences of the United States of America. 1998; 95(26): 15603–7. [PubMed: 9861016]

59. Gehrig SM, van der Poel C, Hoeflich A, Naim T, Lynch GS, Metzger F. Therapeutic potential of PEGylated insulin-like growth factor I for skeletal muscle disease evaluated in two murine models of muscular dystrophy. Growth hormone & IGF research: official journal of the Growth Hormone Research Society and the International IGF Research Society. 2012; 22(2):69–75.
60. Jacquemin V, Furling D, Bigot A, Butler-Browne GS, Mouly V. IGF-1 induces human myotube hypertrophy by increasing cell recruitment. Experimental cell research. 2004; 299(1):148–58. [PubMed: 15302582]
61. Grillet, AM., Wyatt, NB., Gloe, LM. Polymer Gel Rheology and Adhesion. In: De Vicente, J., editor. Rheology. Rijeka, Croatio: InTech; 2012. p. 59-80.
62. Picout DR, Ross-Murphy SB. Rheology of biopolymer solutions and gels. The Scientific World Journal. 2003; 3:105–21. [PubMed: 12806124]
63. Cilurzo F, Selmin F, Aluigi A, Bellosta S. Regenerated keratin proteins as potential biomaterial for drug delivery. Polymers for Advanced Technologies. 2013; 24(11):1025–1028.
64. Gillespie JM. The fractionation of S-carboxymethyl kerateine 2 from wool. Australian Journal of Biological Sciences. 1956; 10(1):105–117.
65. Tannoury CA, An HS. Complications with the use of bone morphogenetic protein 2 (BMP-2) in spine surgery. Spine J. 2014; 14(3):552–9. [PubMed: 24412416]

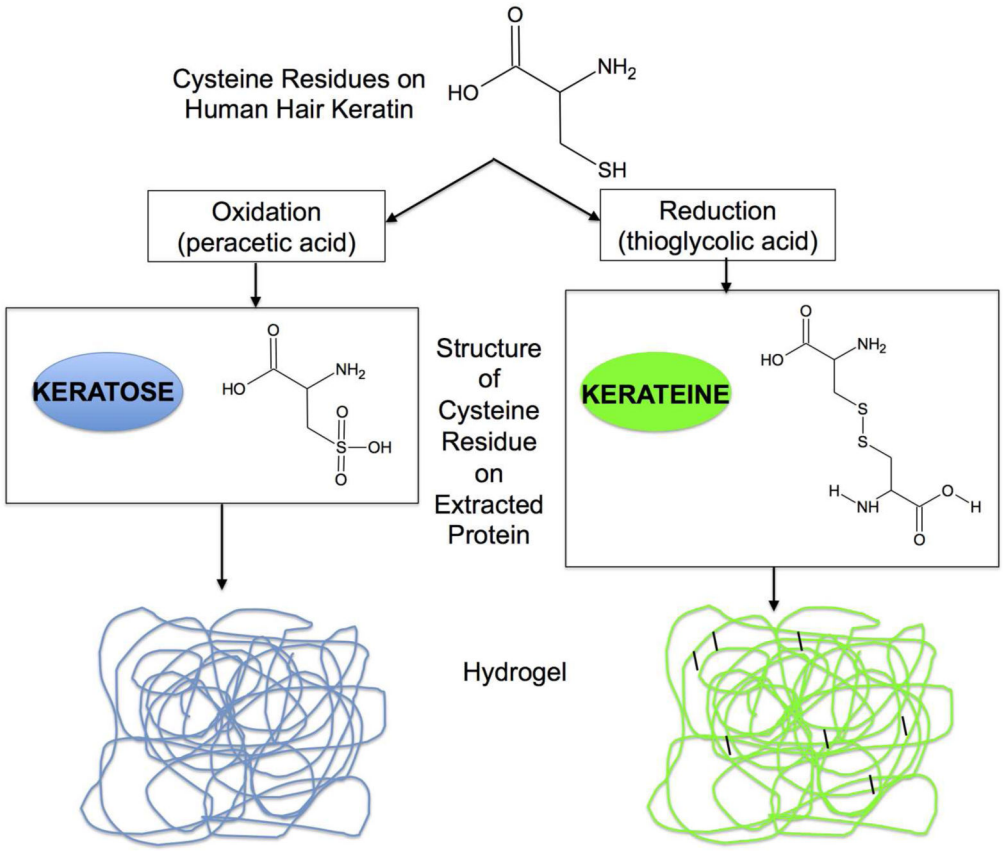

Figure 1.

A simplified schematic of the process for extraction of keratin proteins through oxidative or reductive extraction approaches starting with human hair as the source of keratin. Shown are the chemical structures of cysteine residues initially containing sulfhydryl groups in hair. Following oxidative extraction, keratin is in a form known as keratose (left side) and the cysteine residues contain sulfonic acid “caps” on sulfur groups. This prevents disulfide cross-linking, and resulting hydrogels are held together strictly through chain entanglement. Following reductive extraction (right side), the cysteine residues are not capped and can form disulfide cross-links (either intramolecular or intermolecular). The resulting hydrogels then contain both physical entanglements and covalent (disulfide) cross-links.

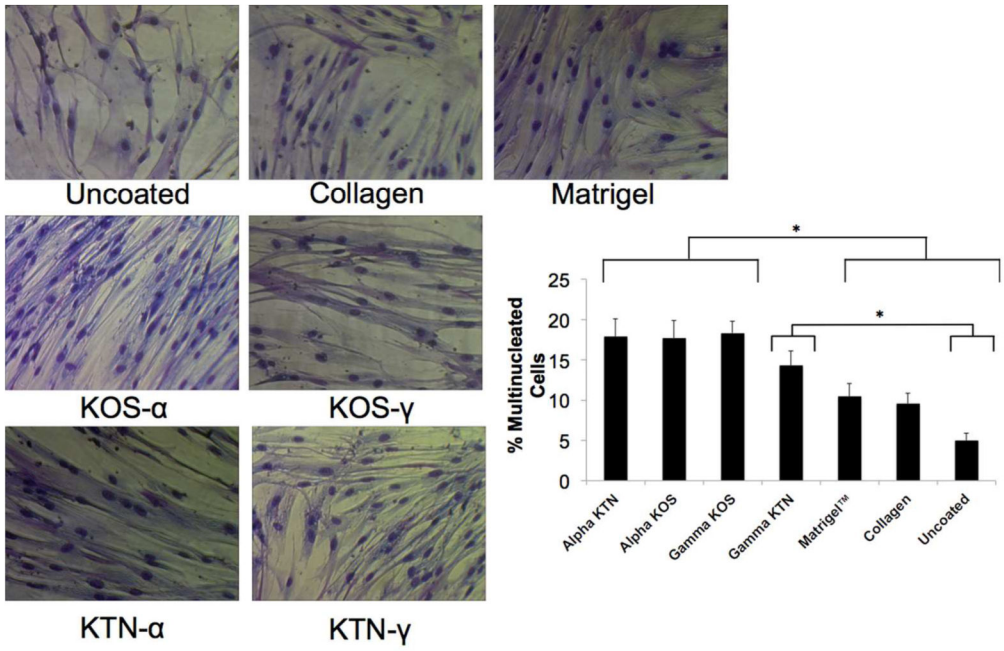

Figure 2. Giemsa staining of hSMM cultured on various coatings

hSMM were cultured on keratin, Matrigel™, collagen or tissue culture plates and after 4 days Giemsa staining was performed (Sigma, St. Louis, MO). The percentage of multi-nucleated cells was determined by counting 20 different fields and determining the percentage of multi-nucleated cells in each as determined by two different individuals. Error bars indicate standard error of the mean. * indicates $P < 0.05$ as determined by one-way ANOVA with Tukey's post-hoc test.

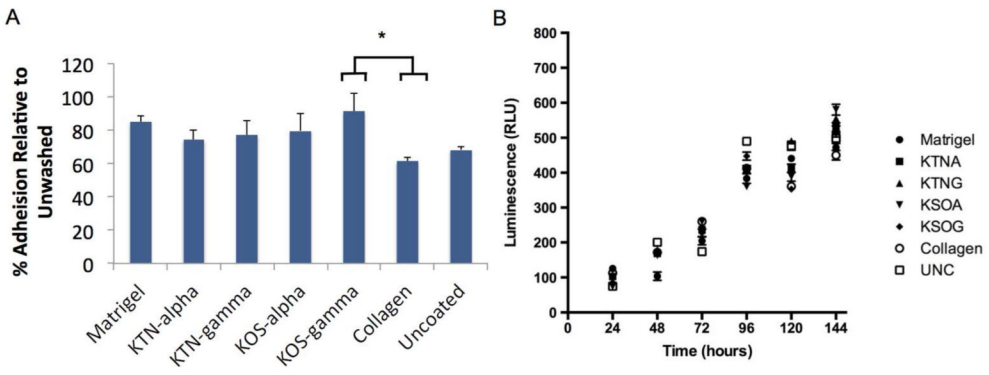

Figure 3. Adhesion and proliferation assays for hSMM seeded on four different keratin coatings, collagen, Matrigel™ and uncoated plates

(A) Adhesion was measured using the Vybrant Group comparison, six replicates per group showed significant difference between keratose gamma and collagen as indicated by the * ($n=6$, $p<0.05$ as determined by one-way ANOVA with Tukey's post-hoc test) Error bars represent SEM. (B). Proliferation was measured at six time points using luminescence measured in light units. No significant differences were shown with single factor ANOVA on proliferation assay in any groups (n=6 per group). Error bars represent SEM.

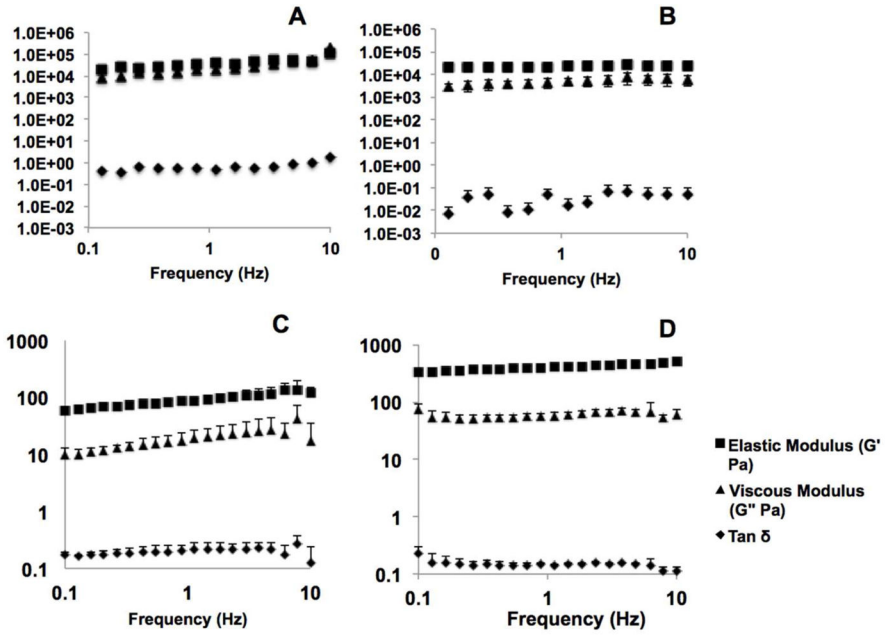

Figure 4.

Rheological characterization of (A) 20% KOS hydrogels, (B) 20% KTN hydrogels, (C) 12% KOS hydrogels and (D) 8% KTN hydrogels as determined by a frequency sweep for the elastic modulus (G′), viscous modulus (G″) and tan δ. Both types of keratin hydrogels show near independence with frequency and a tan δ value of less than 1, indicating the formation of stable hydrogels. The viscous modulus for KTN exhibits less dependence with frequency than KOS, and both G′ and G″ are approximately an order of magnitude higher in KTN than KOS (note the log-log nature of the plot), likely due to the presence of disulfide crosslinks with the material. Error bars denote standard deviation.

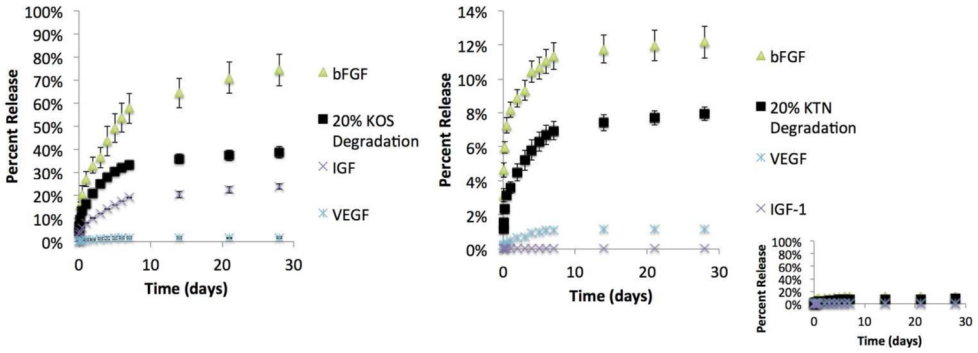

Figure 5. Release of growth factors from keratin hydrogels

Release of bFGF, VEGF, and IGF-1 were determined by ELISAs specific to each growth factor. The rate of degradation of the keratin gels (A. keratose or B. kerateine) are shown as determined by DC protein assay to show correlation between rate of release and keratin hydrogel degradation rate. Please note the differences in scale between keratose (A) and kerateine (B). Inset shows release from kerateine on same scale as keratose to demonstrate the large Keratin hydrogel carrier system difference in release. Error bars are standard deviation, but are too small to see on the graph in some locations.

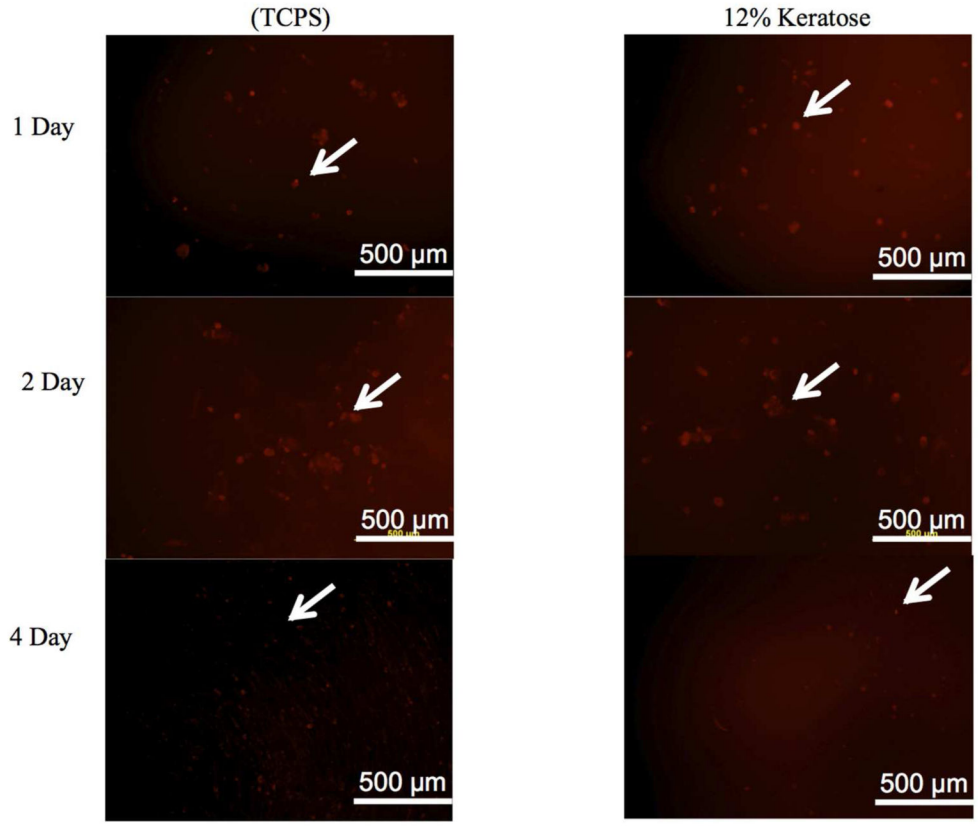

Figure 6. Viability of MPCs in keratose hydrogels in vitro

Fluorescence microscopy images of rat MPCs stained with LavaCell on tissue culture polystyrene (TCPS) or in keratose hydrogels (12% w/v). At 1, 2, and 4 days, MPCs in keratose hydrogels had similar levels of viability as MPCs cultured on TCPS. White arrows highlight the presence of viable cells in the in vitro system.

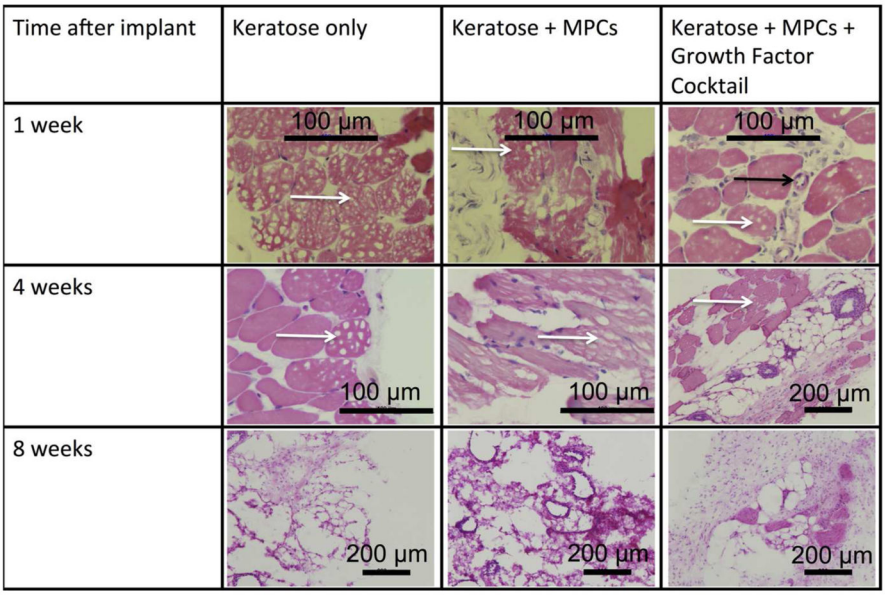

Figure 7. H&E images of explanted keratose hydrogels

Keratose hydrogels were removed at 1, 4, and 8 weeks. Representative H&E images from the keratose only, keratose loaded with MPCs, and keratose loaded with MPCs and growth factors. There were no signs of inflammation. Cells were observed within the keratin hydrogel at 1 and 4 weeks that were consistent with blood vessel and muscle progenitor cells. At the 8 week time point the keratose only group had degraded and was replace with morphology consistent with normal tissue in the subcutaneous space, while the cell loaded keratose was replaced with a highly vascularized, mix of cell consistent with the morphology of muscle progenitor cells. Black arrow indicates location of a blood vessel while white arrows indicate the presence of keratose gel remaining at the implant site. Scalebars are as indicated in the figure.

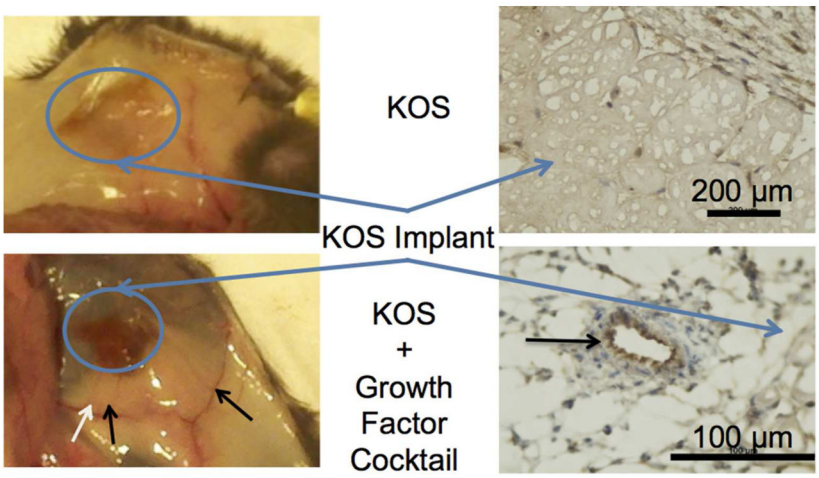

Figure 8. Evidence of VEGF bioactivity by gross observation

Vascularization of the keratose implants could be observed as early as 1 week in the gross examination of the subcutaneous space. Staining of the frozen section with von Willebrand factor confirms the presence of endothelial cells.

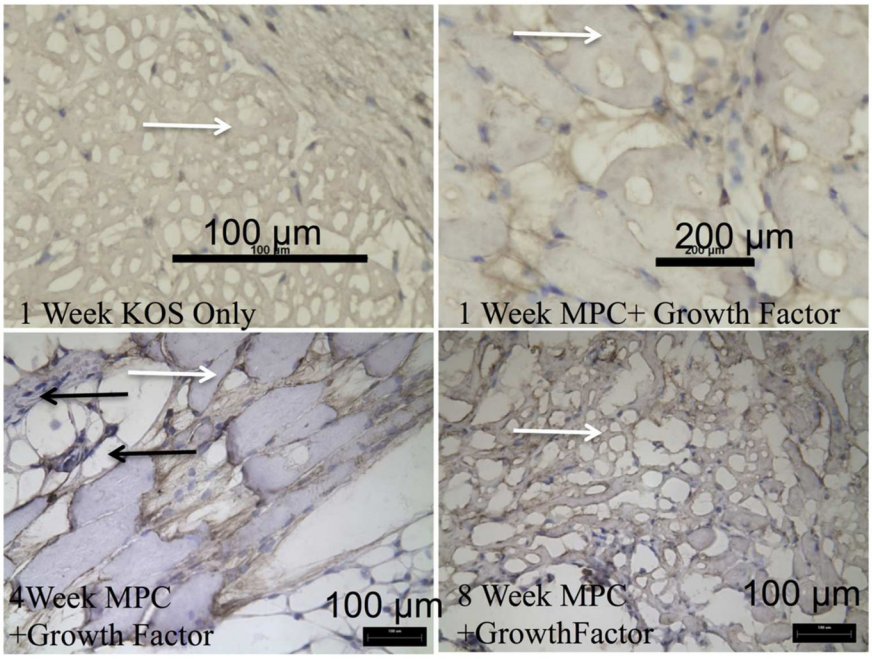

Figure 9. Evidence of skeletal muscle by desmin stain

Tissue sections were stained utilizing an anti-Desmin antibody. Keratose only explants revealed no desmin positive staining cell within the hydrogel. Positive staining for desmin was observed in all keratose samples containing MPCs. As time increased the hydrogel was degraded and replaced with desmin positive cells. White arrows indicate the presence of KOS gels while black arrows indicate desmin positive cells at the 4 week time point.